ARTICLES

Fluorescence of Retinal Schiff Base in Alcohols

Sergei M. Bachilo*

Institute of Molecular and Atomic Physics, F. Skaryna Ave. 70, 220072 Minsk, Belarus

Tomas Gillbro

Department of Chemistry, Biophysical Chemistry, Umeå University, 901 87 Umeå, Sweden

Received: September 9, 1998; In Final Form: December 31, 1998

Spectra, quantum yields, and kinetics of the unprotonated *n*-butyl Schiff base of retinal (SBR) fluorescence are investigated in *n*-alcohols at room temperature. While the absorption spectra in H-bonding solvents are only slightly shifted to longer wavelengths compared to the absorption in hexane, the emission spectra are strongly influenced by H-bond formation. The radiative S_1 state lifetimes are found to be in the 100−200 ns range, indicating that the $S_1 \rightarrow S_0$ transition is strongly forbidden. With decreasing polarity the rate of the S_1 state decay decreases and in pure alcohols the rate exhibits an exponential dependence on the dielectric constant. Semiempirical calculations indicate a larger probability of proton transfer from alcohol to SBR in the excited state than in the ground state, which may result in protonation of the SBR upon excitation. The theoretical model also shows that the polar environment increases the probability of such a proton transfer from alcohol to SBR. The observed experimental results can be explained by an increase of the S_1 state lifetime by H-bonding. Within the model an increase of solvent polarity makes the nonradiative decay faster in the H-bonded complex due to proton transfer from the alcohol to SBR.

Introduction

The Schiff base of retinal (SBR) is a model of the chromophore in different retinal−protein complexes, which are responsible for a large variety of photobiological processes. Examples of such biosystems are rhodopsin and other rhodopsin-like proteins, active in almost all known forms of vision,[1,2] bacteriorhodopsin, which performs charge separation in the non-chlorophyll photosynthesis in *Halobacterium halobium*,[1−3] and halorhodopsin, which transports chloride ions.[4] In these and many other photobiological systems the retinoid molecule is the only chromophore,[2,5,6] which absorbs the light energy and initiates the subsequent dark processes. In all models the function of the polyene chromophore in the photoactive retinoid proteins includes either a proton transfer from its original position to a new site or switching due to deprotonation, that resuls in an electrochemical signal across the biological membrane[6,7] and/or a conformational change of the membrane.[2,8,9] An external proton bound to a SBR molecule in a retinoid−protein complex can play several important roles. First, it induces a spectral shift adapting the pigment absorption into a useful range.[10] Second, it can prevent random and nonspecific isomerization of SBR by locking its ground state conformation.[11] Finally, the proton can be transferred to a new location, or deprotonation can serve as a switch for a proton transfer,[12] that will create a charge gradient in bacteriorhodopsin photosynthesis and stimulate some other photoprocesses.[7−9] Although a conclusive answer about the kind of the link between the SBR nitrogen atom and an external proton is still missing, the model with a very strong N−H bond in the ground state, correlating with the term "protonated SBR" (PSBR), is the most acceptable for bacteriorhodopsin and rhodopsin.[2]

The absorption spectra of natural retinoid proteins cover the entire visible spectrum and even slightly longer wavelengths.[2,11] However, SBR in solvents absorbs in the near-UV range, and the absorption spectrum of PSBR in solvents is strongly shifted to longer wavelengths relative to the spectrum of unprotonated SBR.[2] The protonation shift can explain a large amount of the absorption shift in the chromophore−protein complexes as compared to the SBR absorption, but to describe the longer wavelength absorption of natural proteins maxima a model with a specified protein cavity field must additionally be involved.[11]

Investigation of retinoid protein fluorescence is very complicated. Retinoid proteins have very weak[13−15] and ultrafast fluorescence[16−19] because of excited-state photochemical reactions, the most important one among them is the cis−trans or trans−cis isomerization.[2,16] Together with the ultrafast excited-state dynamics, there is one more difficulty in the retinoid photophysics. Symmetric polyenes with more than three double bonds have a forbidden S_1-S_0 ($2A_g-1A_g$) transition,[20] while the lowest optically active $1B_u$ state is slightly higher. The model is also applicable for SBR in solutions, where the ∼ 200−400 ns radiative lifetime and relatively fast decay of the S_1 state in SBR (∼40 ps) results in a low-fluorescence quantum yield of $\sim 10^{-4}$.[21] The S_1-S_0 transition character is different for PSBR, which has a much lower $1B_u$ energy. However, the S_1 lifetime

* Corresponding author. Current address: Department of Chemistry, MS-60, Rice University, 6100 Main Street, Houston 77005. E-mail: bachilo@rice.edu.

10.1021/jp983646a CCC: $18.00
Published on Web 03/27/1999

TABLE 1: Absorption (λ^a_{max}) and Fluorescence (λf_{max}) Maxima and the Fluorescence Lifetimes (τ_f) and Quantum Yields (Φ_f) for SBR) in Several Solvents and PSBR in Hexane[a]

solvent	n	ϵ	λ^a_{max}, nm	λf_{max}, nm	τ_f, ps	k_d, 10^9 s^{-1}	Φ_f, 10^{-4}	k_f, 10^6 s^{-1}	k_a, 10^6 s^{-1}
hexane	1.375	1.88	356	510	38 ± 3	26 ± 2	0.8 ± 0.2	2.1 ± 0.5	800
methanol	1.329	32.6	362	640	21 ± 3	48 ± 7	2.0 ± 0.2	9.5 ± 1.5	
ethanol	1.361	24.3	363	610	56 ± 4	17.9 ± 1.5	3.5 ± 0.3	6.3 ± 0.7	830
propanol	1.386	20.1	365	605	83 ± 5	12.0 ± 0.7	4.3 ± 0.4	5.2 ± 0.5	
butanol	1.399	17.1	366	600	103 ± 5	9.7 ± 0.4	5.6 ± 0.5	5.4 ± 0.5	
pentanol	1.410	13.9	366	600	129 ± 5	7.8 ± 0.3	7.0 ± 0.6	5.4 ± 0.5	
heptanol	1.425	11.8		600	145 ± 5	6.9 ± 0.2			
decanol	1.437	8.1		600	171 ± 6	5.8 ± 0.2	9.1 ± 0.7	5.3 ± 0.5	
acetonitrile + butanol (vol 4:1)		~33	362		20 ± 3	50 ± 8			
tetradecane + butanol (vol 4:1)		~5		600	200 ± 7	5.0 ± 0.2			
hexane (PSBR)	1.375	1.88	457	620	<6	>160 ~500 [1]	1.8 ± 0.2	>30 ~80[b]	400

[a] The experimental radiative rates ($k_f = \Phi_f/\tau_f$) and calculated radiative rates for the absorption transition (k_a from ref 21), as well as solvent refractive index n and dielectric constant ϵ are also shown. [b] Using 2.3 ps lifetime from ref 23.

in PSBR is substantially shorter than for SBR (~2−5 ps[22−24]) and this neutralizes the increase of radiative rate intensity upon protonation. The short lifetime therefore explains why the PSBR emission quantum yield is also low (~2×10^{-4} in hexane[21]). The presence of two close-lying excited states with different electronic and structural properties leads to problems in experimental and theoretical investigations of the retinoid excited states.

Most recently, a series of theoretical investigations of SBR[25] and similar model systems[26] were used to describe the conformation and isomerization of SBR in the ground and excited states. However, there is an obvious lack of experimental information about proton−SBR interaction, especially in the excited states. This restrains a deeper understanding of the primary processes in retinoid−protein systems. It is also clear that investigations of the system with an intermediate strength of the N−H bonds, which can more easily be modified to reveal the changes occurring upon excitation, will be useful to understand the role of a proton in the excited-state photochemical processes. During the retinoid protein photocycle the proton−SBR bond varies from strongly protonated (PSBR) to completely unprotonated SBR. The evolution must be controlled by the excited-state properties, as well as by the environment.

In the present work, we have investigated the most common case of a SBR molecule linked to an extra proton. This case is hydrogen (H) bonding, where the proton is provided by an external molecule of alcohol. It is well-known that SBR in alcohols exists as the hydrogen-bonded complex (H−SBR) and its absorption spectrum is slightly shifted to longer wavelengths from the absorption of SBR,[27] but not nearly as much as for PSBR. We have studied the fluorescence of SBR in different alcohols and their mixtures with hydrocarbon solvents and compared it to the fluorescence behavior in aprotic solvents. The correlation between fluorescence intensity and lifetime shows the great influence of H-bond formation on the S_1 state properties. While the SBR fluorescence in aprotic solvents did not show a large solvent dependence,[21] H-bonded SBR was strongly influenced by the solvent and the main aim of this work was to understand the solvent effects on the H−SBR emission.

Materials and Methods

The purified crystalline 6s-cis *all-trans-n*-butylamine Schiff base of retinal (SBR) was a gift from Dr. A. Khodonov (Moscow State Academy of Fine Chemical Technology). The compound was stored in the dark at ~200 K or at ~273 K under vacuum. Spectroscopic or reagent grade solvents were usually utilized without further purification. Linear 1-alcohols were used in the work. Freshly prepared solutions were studied in all measurements at ambient temperature ~293 K. The presence of oxygen did not influence the results. Because of the relatively low stability of SBR solutions, fresh samples were used within 1−2 h after preparation. The sample absorption before and after measurements was carefully controlled.

Absorption spectra were measured by a Beckman DU-70 spectrometer. The fluorescence and fluorescence excitation spectra were recorded by a Spex Fluorolog 112 instrument equipped with a cooled Hamamatsu R 928 photomultiplier. The optical densities of the samples in 1 cm quartz cuvettes were typically 0.15−0.4 at the excitation wavelength. As a standard for the SBR fluorescence yield measurements, 1,8-diphenyl-octatetraene in nondegassed *n*-hexane ($\Phi_f = 0.02$[28]) was used. Weak background emission and solvent Raman scattering were subtracted from the spectra. The spectra were also corrected for the instrument emission and excitation sensitivity.

Measurements of the fluorescence kinetics were performed by a time-correlated single photon counting system equipped with a microchannel plate R2609U-05 (Hamamatsu Photonics), an ORTEC 567 time-to-amplitude converter and a Nucleus personal computer analyzer. Excitation light in the 370−390 nm and 410−430 nm ranges was obtained by frequency doubling a dye laser emission (Styryl 8 and Styryl 9 dyes) with a $LiIO_3$ crystal. The dye laser was synchronously pumped by a CW Nd:YAG laser (Spectra Physics). The excitation pulse duration was about 10 ps, and a repetition rate of 0.8 or 4 MHz was used. The average power at the sample was below 0.5 mW, and the illuminated sample area was ~2 mm^2. A thin $\lambda/2$ retardation plate in the excitation beam turned its polarization to any desired direction. The spectral width of the monochromator slits was 8−16 nm. To increase the system sensitivity, some kinetic traces were measured with red cutoff filters instead of the monochromator.

For the kinetic measurements the samples were usually placed in 1 cm quartz cells and the optical densities of the solutions were from 2 to 6 to ensure the excitation pulse absorption within a short path, thus preventing a possible decrease of the system resolution (1 mm in toluene corresponds to 5 ps). The emission was collected from the front or side wall of the cell in direction perpendicular to the excitation beam. Additional color glass filters were used to avoid scattered light. The instrument response function was recorded at the excitation wavelength from a scattering sample or the sample under investigation. During every experimental series the response function was stable and had a full width at half-maximum (fwhm) of 50−60 ps. Reconvolutions of the emission kinetics and the fluorescence anisotropy kinetics were performed by our own program. The time-resolution limit was found to be about 5 ps for a one-

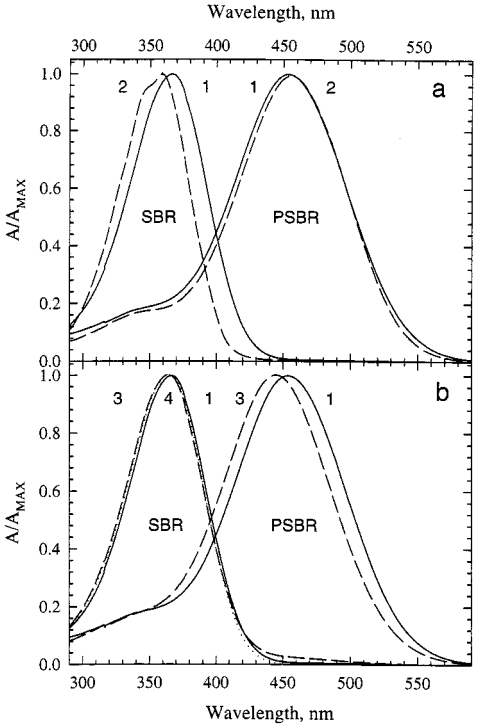

Figure 1. Normalized absorption spectra of SBR and PSBR in butanol (1, solid line, a and b), hexane (2, dashed line, a), methanol (3, dashed line, b), and in butanol + hexane (vol 1:3) mixture (4, dotted line, b).

exponential decay. Calculations with up to three exponential components were used in the present work.

Results and Discussion

The absorption and fluorescence maxima in hexane and different alcohols are given in Table 1. Examples of absorption spectra of SBR and PSBR in hexane and alcohols are shown in Figure 1. All the spectra are very broad and show a lack of structure. Only the absorption spectrum of SBR in hydrocarbons exhibits a weak structure (Figure 1), which is reduced by solvents with larger refractive index and completely disappears upon H-bonding and protonation. The formation of the H-bonds between SBR and alcohol provides a large part of the bathochromic shift of the SBR absorption from hexane to alcohol, which is about 450 cm^{-1}. Besides the H-bond associated shift, there is an additional small shift in the alcohol series, and the absorption maxima in alcohols with longer hydrocarbon chains are shifted to longer wavelengths. This could be a result of decreasing dielectric constant (solvent polarity) or, more likely, increasing refractive index (solvent polarizability). It is well-known that polyene absorption moves to longer wavelengths with an increase in the refractive index.[20] The total absorption shift is substantially smaller than the shift due to protonation, which is ~20 times larger (Figure 1a). An addition of a relatively small amount (~10%) of alcohol to the hydrocarbon solvent also resulted in complete formation of H−SBR exhibiting the corresponding absorption spectrum (an example with 25% of butanol in hexane is shown in Figure 1b).

In contrast to the absorption spectra, the fluorescence spectra show a very strong shift (~4000 cm^{-1}) from hexane to methanol (Figure 2, Figure 3, Table 1). The emission shift within the alcohol series is in the opposite direction to the absorption shift, with a blue shift from methanol to decanol of ~1000 cm^{-1}. It is noteworthy that the pronounced fluorescence shift within the alcohol series is only observed in the case of the shortest alcohol molecules, methanol and ethanol, while in longer-chain alcohols

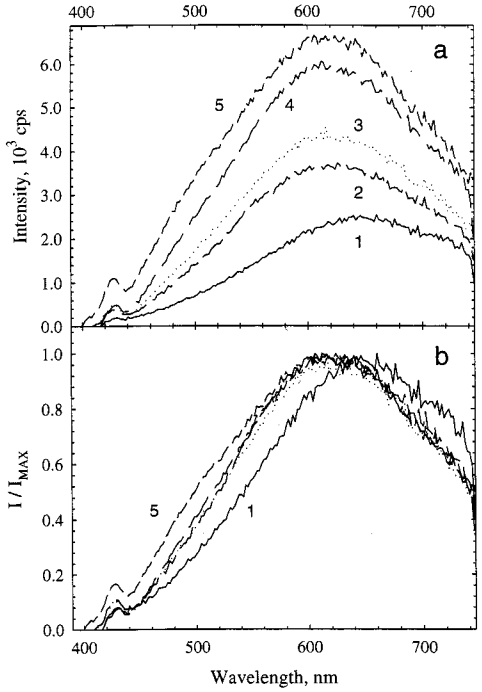

Figure 2. Fluorescence (a) spectra of SBR in methanol (1), ethanol (2), propanol (3), butanol (4), and in butanol + tetradecane (vol 1:1) mixture (5). Part b shows the same spectra normalized at the maximum.

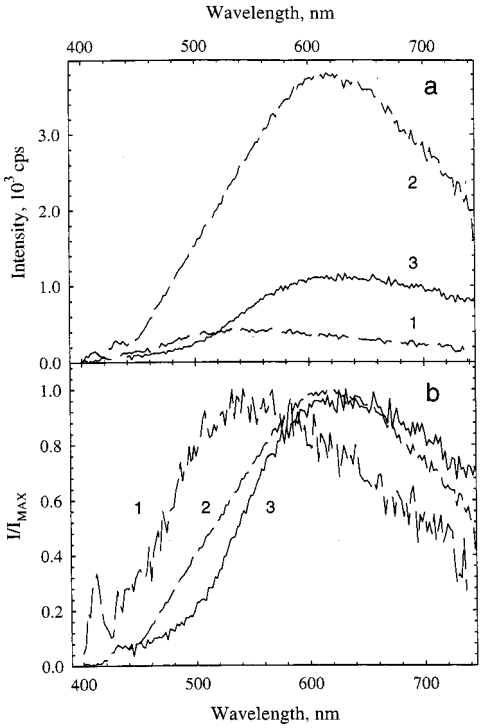

Figure 3. Fluorescence spectra of SBR in tetradecane (1) and butanol (2), and the PSBR fluorescence spectrum in tetradecane (3). Part b shows the same spectra normalized at the maximum.

the fluorescence maximum is practically invariable (~600 nm, Figure 2b, Table 1). The H−SBR emission intensity increases with the size of the alcohol molecule and, correspondingly, with decreasing the alcohol polarity, as well as with decreasing polarity for solvent mixtures. In general, the spectral shape of the H−SBR fluorescence is closer to that of the PSBR fluorescence than to the SBR fluorescence spectrum (Figure 3b). However, the quantum yield of the H−SBR fluorescence is

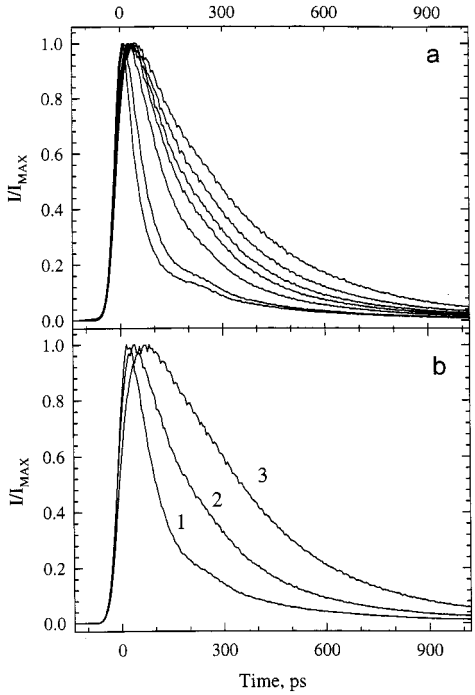

Figure 4. Fluorescence kinetics of SBR in a set of alcohols (a, methanol, ethanol, propanol, butanol, pentanol, heptanol, and decanol, in order of increasing lifetime). Part b shows the SBR kinetics in butanol + acetonitrile mixture (1), in pure butanol (2), and in butanol + hexane mixture (3).

higher than the quantum yields of the PSBR and SBR fluorescence in aprotic solvents (Figure 3a, Table 1).

Examples of kinetic traces of the H−SBR fluorescence in different alcohols, as well as in mixtures of alcohols with aprotic solvents, are shown in Figure 4. Fitting of the fluorescence kinetics indicates that the decays contain a single dominant component with duration from 20 to 200 ps (Table 1). For some solvents the second weak component (<3%) can be observed in the nanosecond scale (2−4 ns lifetime), although it is negligible for the most polar alcohols. The relative amplitude of this nanosecond component decreases with increasing emission wavelength and it can be attributed to impurities. The presence of an impurity tail is common in kinetics of weakly emitting compounds and the very low relative weight indicates the high purity of the samples studied. For the main picosecond components, no dependence on emission wavelength is found. For the long-chain alcohols (from heptanol to decanol) the decay can be better described by two- and three-exponential curves with slightly different lifetimes and comparable weights. The ratio of the longest lifetime to the shortest one is below 2 in a three-component model and even smaller in the two-component approximation. As a result, the accuracy of a multicomponent fit is just slightly better than that of a one-exponential approximation. Due to a small lifetime difference we cannot clearly distinguish between the monoexponential model and two- or three-component models or even a narrow lifetime distribution. The nonexponential decay in these solvents can be a result of dynamic structural inhomogeneity of the local solvent environment arising from the higher solvent viscosity. Table 1 contains the fluorescence lifetimes calculated for the set of alcohols in the one-exponential model.

As was observed earlier,[21] the excited state lifetime of unprotonated SBR is insensitive to solvent properties for the case of aprotic solvents. It is almost constant in hexane, toluene, highly polar acetonitrile, and viscous paraffin oil. But for alcohols a pronounced lifetime dependence on the alcohol length has been observed (Figure 4, Table 1). The increase of the fluorescence quantum yield is approximately proportional to the lifetime increase for all alcohols except methanol, and the radiative lifetime is thus almost constant for long alcohols (Table 1). Only in the case of the most polar solvents, methanol and ethanol, are higher radiative rates calculated. The SBR radiative rate in long alcohols is about 2 times higher than in hexane. However, these radiative rates are still more than 2 orders of magnitude lower than the radiative rates calculated from the SBR absorption spectrum with the Strickler−Berg equation (Table 1). This means that the polyene two-level model of the lowest excited states[20] is also applicable to H−SBR. In this model the S_1 state has the A_g symmetry and the dipole transition between the S_1 and the ground A_g state is forbidden and, accordingly, very weak. The close-lying S_2 state has B_u symmetry and it is responsible for the absorption. The S_2 state can provide a radiative rate of about 10^9 s^{-1}, as calculated from the most intense absorption band (Figure 1, Table 1).

Considering the excited state order in SBR, it is noteworthy to mention that the decrease of the $1B_u$ state energy in PSBR, corresponding to the large bathochromic shift of its absorption, can essentially change the state ordering. In PSBR the $1B_u$ state can be even lower than the $2A_g$ state or, most likely, the states are very strongly mixed and cannot be clearly distinguished. As a result, for PSBR the ratio of the radiative rates, determined from its absorption spectrum and experimental fluorescence yield and lifetime, is still different, but the difference is much lower as compared to SBR (Table 1). On the other hand, hydrogen bonding produces just a small shift of the absorption spectrum ($1B_u$ state) and the lowest excited state ordering should be close to that of SBR in aprotic solvents, at least in the ground state conformation.

The logarithm of the H−SBR fluorescence lifetime can be satisfactorily fitted by a linear dependence on the solvent dielectric constant. But the best simple fit is provided by the "shifted" equation $k(\epsilon) = k_0 + A \exp(\alpha \epsilon)$, where $k(\epsilon)$ is the decay rate and A and α are the fitting parameters (Figure 5). Since the solvent dielectric constant is a measure of the solvent polarity, we shall consider the influence of the environmental polarity on the lifetime. The almost constant radiative rate calculated for most of alcohols indicates that increasing polarity results in the substantial increase of the nonradiative decay and just slightly influence the radiative rate. The $k_0 + A$ value is very close to the radiative rate of H−SBR in solvents with low polarity, where $\exp(\alpha\epsilon) \approx 1$. Such a system could be prepared as a mixture of alcohols with hydrocarbon solvents. In the solvents with a small (down to 10%) volume of long-chain alcohol the emission lifetime is 200−220 ps (results for a mixture with 25 vol % of butanol are shown in Figure 4b and Table 1). In these low-polar mixtures the highest value for the fluorescence quantum yield, as well as the emission spectrum maximum at the shortest wavelength, are found. On the other hand, an addition of a very polar aprotic solvent, such as acetonitrile, to an intermediate polar alcohol (butanol) essentially decreases the SBR fluorescence lifetime, as well as the fluorescence quantum yield (Figure 4b). In the mixture containing a large amount of acetonitrile the fluorescence lifetime is the same or even shorter than in pure methanol. This is likely related to the high polarity ($\epsilon = 37$) of acetonitrile, resulting in the high polarity of the mixture (Table 1).

The fluorescence decay is not sensitive to the solvent viscosity. For example, in the alcohol−alkane mixtures mentioned above, there is no detectable lifetime difference upon replacement of hexane by tetradecane or paraffin oil. Thus, we

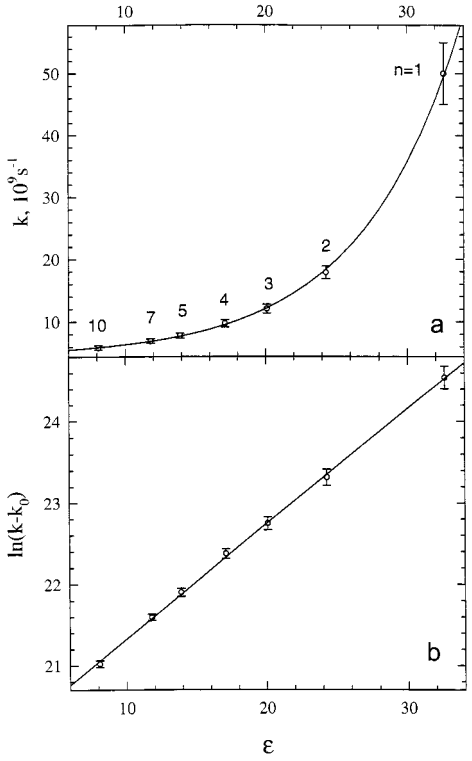

Figure 5. Dependence of the fluorescence decay rate, k, for SBR in alcohols $C_nH_{2n+1}OH$ on the solvent dielectric constant, ϵ. Part b illustrates the dependence on a shifted logarithmic scale. The solid lines show the following fit: $k = k_0 + A \exp(\alpha\epsilon)$, where $k_0 = 4.5 \times 10^9\ s^{-1}$, $A = 4.42 \times 10^8\ s^{-1}$, $\alpha = 0.142$.

may conclude that the environment polarity is the dominant factor influencing the fluorescence lifetime in H-bonded SBR. Other individual properties of solvents, including the solvent viscosity, do not noticeably affect the kinetics when H−SBR has been formed.

Semiempirical calculations (AM1 and PM3 methods, HyperChem version 4.0, HyperCube, Inc.) have been applied to test the interaction of SBR with alcohols. The systems containing a SBR molecule and several alcohol molecules near the SBR N atom have been optimized in the ground state. Formation of only one hydrogen bond between the alcohol and SBR molecules has been found. After the optimization, the ground- and excited-state energies can be calculated (PM3, configuration interaction, 99 single excited conformations were used) for different intermediate positions of the proton between the alcohol O atom and the SBR N atom (Figure 6, Figure 7). The H-bond strength is found to be practically the same for different alcohols for the case of one alcohol molecule in the system. The potential surfaces for the proton transfer (Figure 7b) indicates that the ground-state proton replacement from the alcohol oxygen to the SBR nitrogen is not possible, because the ground state the form with a proton near the N atom (the protonated-like form, Figure 6B) has much higher energy than the "normal" H−SBR (Figure 6A). However, upon increasing the number of methanol molecules near the SBR N atom, the possibility of the proton transfer in the ground state increases (Figure 7b). A different picture is found for the B_u-like excited state (Figure 7a). As follows from the potential surface, the proton can more easily be displaced from the alcohol oxygen to the SBR N atom due to lowering the relative energy of the excited-state protonated-like form. The probability of the excited-state proton transfer also increases with the number of alcohol molecules, mainly due to the decrease of the protonated-like form energy in the ground state, while the transition energy between the ground

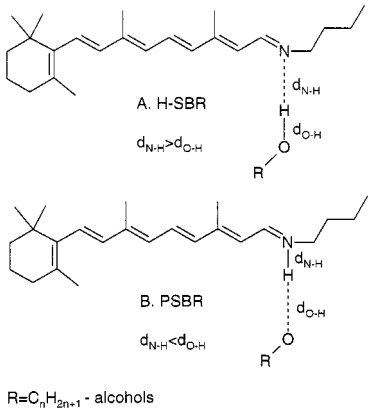

Figure 6. Chemical structure of H−SBR (A) and the protonated-like form (B) with an external alcohol molecule.

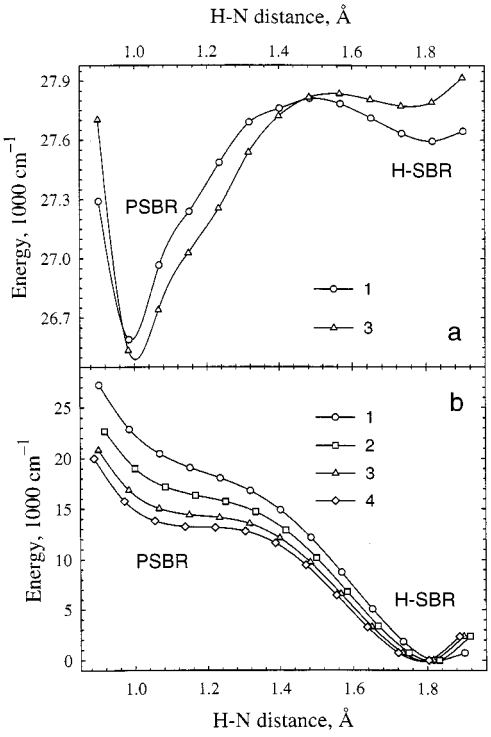

Figure 7. Potential surfaces for the ground (b) state and the relative energy of the excited state (a) for the SBR−methanol complexes with the different numbers of alcohol molecules. PSBR denotes the protonated-like form (the proton is near the nitrogen atom), H−SBR is the hydrogen-bonded complex (the proton is closer to the oxygen atom). Calculated with the PM3 method.

and $1B_u$ states was not substantially changed. Thus, an increase of the number of alcohol molecules near the H-bonded alcohol molecule was applied to simulate an increase of the local environment polarity. The rise of the number of methanol molecules resulted in an increase of the N−H hydrogen bond strength. Formation of external alcohol−alcohol hydrogen bonds also makes the O−H bond in the N−H−O line weaker.

Thus, the N−H distance decreases, corresponding to the motion of the equilibrium conformation on the potential surface toward the protonated-like form (Figure 7b). For the small number of alcohol molecules that correspond to ambient polarities of the environment, the absorption transition energy is just slightly sensitive to the polarity. However, the barrier for the ground-state proton transfer is decreasing with the polarity increase. The barrier lowering can likely be observed in formation of small concentration PSBR in a case of methanol solutions. Because of the lower energy of the protonated-like

form in the excited $1B_u$ state, the probability of the proton transfer can be much higher in this excited state.

The shown semiempirical results should not be considered as complete for the excited state, because in the case of H−SBR the polyene system has an additional A_g-like S_1 state, which cannot be determined from the semiempirical model used. However, the results of semiempirical calculations can help to understand the excited-state evolution of SBR in its interaction with an alcohol molecule. The SBR excited state $1B_u$ provides an electron density displacement toward the nitrogen atom and this additional negative charge must result in a stronger attraction between the SBR nitrogen and an external proton. This process results in the substantial red shift of the SBR absorption upon protonation. Consequently, the $1B_u$ state has a much higher possibility to link a proton, and the proton can move toward the nitrogen. The polar environment influences this process by increasing the dipole moment of the polyene chain, because it can induce an additional charge displacement in the ground and excited states. Correspondingly, the ground state bond between the nitrogen atom and the alcohol proton will be stronger and the protonated-like form will more easily be formed. On the other side of the H-bonded complexes, the polar environment will decrease pK_a of the alcohol residue because of neutralizing (screening) of the negative charge of the alcohol oxygen by the polar environment. One such effect is observed as the above-mentioned formation of H-bonds between an alcohol molecule, having a proton linked to SBR, and another situated nearby alcohol molecule. Due to the screening effect, the H-bonded alcohol molecule can lose its proton more easily in a polar environment. This second way of increasing the SBR−proton interaction is probably more important than the induced dipole moment in SBR molecule.

As demonstrated by the semiempirical calculations, there is a possibility of excited-state proton transfer and transformation of the H-bonded SBR to the protonated-like form. Because the PSBR S_1 state has a much shorter lifetime, we can suggest that the proton transfer may be responsible for the quenching of the H−SBR fluorescence with polarity increase. For a more quantitative description let us consider the dynamics of the system with two species in the excited state or two excited levels.

A system of kinetic equations for two excited states can be written as

$$\begin{aligned} dN/dt &= -k_1N_1 - k_{12}N_1 + k_{21}N_2 \\ dN_2/dt &= k_{12}N_1 - k_2N_2 - k_{21}N_2 \end{aligned} \tag{1}$$

where N_1 and N_2 are the level populations, k_1 and k_2 are the deactivation rates of the levels (here they are transitions to the ground state), and k_{12} and k_{21} are the rates of transitions between these two levels. If $E_{21} = E_2 - E_1$ is the energy difference between two levels of the same multiplicity

$$k_{12} = k_{21} \exp(-E_{21}/k_BT) \tag{2}$$

The time-dependent emission spectrum $I(\lambda,t)$, which is the spectral density of the emitted photon rate, can be represented as the following sum:

$$I(\lambda,t) = N_1(t)k_1^e\sigma_1(\lambda) + N_2(t)k_2^e\sigma_2(\lambda) \tag{3}$$

where λ is the wavelength, t is the time, k_i^e are the radiative rates of two levels, and $\sigma_i(\lambda)$ are the spectral shapes of the emission from each level, normalized for the integral of the entire spectrum. Consequently, the total emission spectrum $S(\lambda)$ will be equal to the integral of the kinetics

$$S(\lambda) = k_1^eP_1\sigma_1(\lambda) + k_2^eP_2\sigma_2(\lambda) \tag{4}$$

where P_1 and P_2 are the integrals of the N_1 and N_2 populations. In a steady-state experiment they are always proportional to the average population of the levels. And, as the final point, because the area under spectra $\sigma_i(\lambda)$ is equal to unity, the total intensity of emission, being the total number of emitted photons, is described by the value F

$$F = k_1^eP_1 + k_2^eP_2 \tag{5}$$

Because the second state (we will use it as the PSBR form) is substantially higher than the first one and eq 2, $k_{21} \gg k_{12}$. Also, since only the nonprotonated form can be present in solution in the ground state, this form can be excited. Together with the previous condition this means $N_2 \ll N_1$. We can also consider two further possible simplifications. In the case of a very fast quenching on level 2, we have $k_2 \gg k_1$, $k_2 \gg k_{12}$, the N_2 population is very low, and it is proportional to the N_1 population. The original linear system (1) is then be simplified to the following form:

$$\begin{aligned} N_2 &= \gamma N_1;\ \gamma = k_{12}/k_2 \\ dN_1/dt &= -(k_1 + k_{12})N_1 \end{aligned} \tag{6A}$$

Another simplification occurs if the levels can quickly transform into each other; this means that the transition between the levels is faster than their internal decay, $k_{21} \gg k_2$ and $k_{12} \gg k_1$. In this case (the case of thermodynamic equilibrium) one can get a similar linear system with slightly different coefficients:

$$\begin{aligned} N_2 &= \gamma N_1; \quad \gamma = k_{12}/k_{21} \\ \frac{dN_1}{dt} &= -\left(k_1 + \frac{k_2k_{12}}{k_{21}}\right)N_1 \end{aligned} \tag{6B}$$

Since systems (6A) and (6B) have only one linear differential equation, both levels exhibit a monoexponential decay with the total duration $\tau = 1/(k_1 + \gamma k_2)$, where $\gamma = k_{12}/k_2$ (case A) or $\gamma = k_{12}/k_{21}$(case B). Substituting with τ and γ, the total kinetics (3) are transformed to

$$I(\lambda,t) = N_1(t)\{k_1^e\sigma_1(\lambda) + \gamma k_2^e\sigma_2(\lambda)\} \tag{7}$$

and the total emission spectrum (4) and the emission integral (5) are described by

$$S(\lambda) = P_1\{k_1^e\sigma_1(\lambda) + \gamma k_2^e\sigma_2(\lambda)\} = N_1(0)\tau\{k_1^e\sigma_1(\lambda) + \gamma k_2^e\sigma_2(\lambda)\} \tag{8}$$

$$F = P_1\{k_1^e + \gamma k_2^e\} = N_1(0)\tau\{k_1^e + \gamma k_2^e\} \tag{9}$$

In eqs 8 and 9, we use $P_1 = N_1(0)\tau$, because the integral for any exponential curve is equal to the product of the starting intensity with lifetime.

The value $\Phi_f = F/N_1(0)$ gives the emission quantum yield, because $N_1(0)$ is equal to the number of absorbed photons.

Consequently, the ratio of the quantum yield and lifetime

$$k_e = k_1^e + \gamma k_2^e \tag{10}$$

represents the effective radiative rate of the system.

Equation 7 indicates that for a very fast decay from level 2 or for thermodynamic equilibrium the emission kinetics cannot depend on the detection wavelength. This is in agreement with our experimental observations. While the "internal" coefficients for both forms 1 and 2 (k_1 and k_2) do not depend on the environment, the transition rate k_{12} (or the corresponding k_{12}/k_{21} ratio) does, and it is the only variable parameter. The nondependence of k_1 and k_2 on the environment should correspond in our case to the nondependence of the SBR and protonated-like SBR lifetime on environment. Consequently, the nonradiative decay in H−SBR, $k = 1/\tau$, depends on environment because k_{12} depends on the environment.

The transformation rate k_{12} can vary with the potential barrier height and width, as well as with the energy gap E_{21} between two forms. k_{21} is the rate of the reverse transformation, which depends mainly on the barrier height and width but does not depend on the energy difference (some dependence on the energy difference could be present in k_{21}, but it is negligible compared with the exponential function). For levels with different dipole moments or other polarity-dependent properties, the energy gap E_{21} should depend on the environment polarity. The dielectric constant ϵ is the parameter that describes the screening of the external field by the medium, and this means that the interaction energy of two charges decreases with increasing ϵ.

Thus, we can suppose that the energy gap E_{21} contains a component which is linear with the dielectric constant ϵ, $E_{21} = E_0 + L\epsilon$, where ϵ is the dielectric constant, and L is a coefficient. Then, we have $k_{12} = k_{21} \exp\{-(E_0 + L\epsilon)/k_BT\} = k_{21} \exp(-E_0/k_BT) \exp(-L\epsilon/k_BT)$. Taking the decay rate in (6A) or (6B) one gets $k = k_1 + A \exp(-L\epsilon/k_BT)$, where $A = k_{21} \exp(-E_0/k_BT)$ or $A = k_2 \exp(-E_0/k_BT)$. These equations are equivalent to the fitting function in Figure 5 with $k_1 = k_0$, and the coefficient $\alpha = -L/k_BT$. $k_0 = k_1$ is the internal decay rate on level 1, which is taken as the H-bonded SBR. The decay rate of the excited H−SBR in a nonpolar environment is then equal to $\sim(k_0 + A)$ ($\sim 5 \times 10^9$ s^{-1} from the data in Figure 5).

As follows from eq 9, the fluorescence quantum yield increases together with the lifetime increase. However, the effective radiative rate remains constant until $k_1^e \ll \gamma k_2^e$ (eq 10) and becomes larger only at very fast quenching rates, corresponding to larger values of γ. Such an increase is observed in methanol and ethanol. Since the radiative rate in methanol is about twice as higher as in solvents with very low polarity, we can accept that in this case $k_1^e = \gamma k_2^e$. While the protonated-like form cannot be considered as having exactly the same properties as ordinary PSBR in solvents, it should be similar. Accepting k_1 and k_1^e as parameters for H−SBR in solvents with very low polarity, $\gamma k_2^e = k_f - k_1^e$ and $\gamma k_2 = k - k_1$, which represents the weights of the protonated-like form in the decay rate and in the fluorescence quantum yield. The parameters allow us to determine the emission quantum yield for the protonated-like form within the total system: $\Phi = k_2^e/k_2 = \gamma k_2^e/\gamma k_2$. Thus, $\Phi_2 \approx 10^{-4}$ in methanol. This value is between the SBR and PSBR quantum yield in aprotic solvents and is not very different from them (Table 1). A γ value from 0.05 to 0.1 in methanol and the corresponding values of $k_2^e = (5-10) \times 10^7$ s^{-1} and $k_2 = (5-10) \times 10^{11}$ s^{-1} seem to be applicable for this system.

The observed shift of the fluorescence spectrum to longer wavelengths (Figure 2) can be ascribed to the solvent polarity effect, as well as to the presence of emission of the protonated-like form. In sufficiently polar solvents all molecules will decay through the excited state of the protonated-like form and will show a fluorescence spectrum consisting of the total PSBR fluorescence and the additional H-bonded form fluorescence, as follows from eq 8. If the relative weight of the protonated-like form emission is significant, as in the methanol case, this can induce a bathochromic shift. At very low polarities the relative weight of the protonated-like form is smaller because of the longer lifetime of the H-bonded form emission. Thus, because the emission intensity almost completely (>80%) originates from the H-bonded form in low polar alcohols (from butanol and longer-chain alcohols), we do not observe a noticeable variation of the position of the emission maximum. Furthermore, the radiative rate is also found to be almost constant for these alcohols.

As can be seen from Table 1, the H−SBR emission exhibits slightly higher radiative rates than the SBR emission in aprotic solvent. This is most likely a result of the smaller $2A_g-1B_u$ energy gap and a stronger mixing between the states. Another cause of the radiative rate increase could be the influence of the proton as a charged particle, which could decrease the SBR molecule symmetry. The estimated radiative rate of the protonated-like form is substantially higher than that of the nonprotonated form and it is equal to, or slightly lower than, the "normal" PSBR radiative rate.

In the model considered, the description with thermodynamic equilibrium between H-bonded and protonated-like forms seems to be the most realistic. Such a small particle as a proton can move with rates corresponding to the "normal" frequency of a stretch vibration. This gives a characteristic rate of $>5 \times 10^{13}$ s^{-1} for k_{21}, and this value is substantially higher than k_2 ($<10^{12}$ s^{-1} [23]). We consider two cases to show that the possible differences are not important within the model.

The excited-state proton transfer must also influence the excited-state SBR isomerization. It has been shown that while the yields of trans−cis photoisomerization are very low for nonprotonated SBR in aprotic solvents, the SBR exhibits high yields in protonated form in all solvent studied, as well as in unprotonated form in alcohols.[29−31] Thus, the excited-state protonation can explain the similarity between the photoisomerization of protonated and H-bonded forms of SBR, since the S_1 state of both forms appear to decay as the PSBR S_1 state.

Conclusion

The fluorescence investigation of H−SBR indicates that this form of the SBR molecule has specific photophysical properties, which are different from the properties of SBR in aprotic solvents, as well as from that of PSBR. H−SBR shows an "internal" possibility to have a relatively long-lived S_1 state. However, the presence of the close-lying proton and an increase of the SBR proton-binding ability in the excited-state stimulate the H−SBR S_1 state decay due to the excited-state proton transfer from the alcohol to SBR. Excluding the most polar media, H−SBR shows a fluorescence quantum yield, being higher than the quantum yields of SBR and PSBR. The H−SBR S_1 state lifetime is also longer than that of SBR and much longer than the PSBR S_1 lifetime.

The strong influence of the environment polarity indicates that specific electric fields efficiently influence the photophysics and photochemistry of the SBR molecule with an extra proton. This makes it likely that specific environmental fields in proteins can affect the H−SBR photochemistry more strongly than the randomly distributed solvent molecules. Further experimental

investigations will help to reveal what are the main factors controlling the excited-state protonation. Additional theoretical simulations in this direction can also show the influence of specific external conditions on the probability of excited-state proton transfer in H−SBR and on the following evolution of the protonated-like form.

Acknowledgment. We thank Dr. A. Khodonov for the samples of Schiff base of retinal and Dr. A. Macpherson for the critical reading of the manuscript. We are grateful to the Swedish Institute (S.B.), the Swedish Research Council for Engineering Sciences (TFR), and Carl Trygger Foundation for financial support of the polyene research project.

References and Notes

(1) Oesterhelt, D.; Stoeckenius, W. *Nature* **1971**, *233*, 149.
(2) Birge, R. R. *Biochim. Biophys. Acta* **1990**, *1016*, 293.
(3) Yoshizawa, T.; Wald, G. *Nature* **1963**, *197*, 1279.
(4) Schobert, B.; Lanyi, J. K. *J. Biol. Chem.* **1982**, *257*, 10306.
(5) Ovchinnikov, Y. A. *Photochem. Photobiol*. **1987**, *45*, 909.
(6) Nakanishi, K. *Pure Appl. Chem*. **1991**, *63*, 161.
(7) El-Sayed, M. A. *Acc. Chem. Res*. **1992**, *25*, 279.
(8) Haupts, U.; Haupts, C.; Oesterhelt, D. *Proc. Natl. Acad. Sci. U.S.A.* **1995**, *92*, 3834.
(9) Lanyi, J. K.; Varo, G. *Isr. J. Chem.* **1995**, *35*, 365.
(10) Kakitani, K.; Kakitani, T.; Rodman, H.; Honig, B. *Photochem. Photobiol*. **1985**, *41*, 471.
(11) Barlow, R. B.; Birge, R. R.; Kaplan, E.; Tallent, J. R. *Nature* **1993**, *366*, 64.
(12) Nagle, J. F.; Mille, M. *J. Chem. Phys.* **1981**, *74*, 1367.
(13) Sineschekov, V. A.; Litvin, F. F.*Biophysics* **1976**, *21*, 313 (in Russian).
(14) Doukas, A. G.; Junnarkar, M. R.; Alfano, R. R.; Calender, R. H.; Kakitani, T.; Honig, B. *Proc. Natl. Acad. Sci. U.S.A.* **1984**, *81*, 4790.
(15) Alfano, R. R.; Govinjee, R.; Becker, B.; Ebrey, T. G. *Biophys. J.* **1976**, *16*, 541.
(16) Mathies, R. A.; Lin, S. W.; Ames, J. B.; Pollard, W. T. *Annu. Rev. Biophys. Biophys. Chem.* **1991**, *20*, 491.
(17) Du, M.; Fleming, G. R. *Biophys. Chem.* **1993**, *48*, 101.
(18) Kandori, H.; Yoshihara, K.; Tomioka, H.; Sasabe, H.; Shichida, Y. *Chem. Phys. Lett.* **1993**, *211*, 559.
(19) Bachilo, S. M.; Gillbro, T. *Bacteriorhodopsin fluorescence kinetics*, unpublished work.
(20) Hudson, B.; Kohler, B. *Annu. Rev. Chem. Phys.* **1974**, *25*, 437.
(21) Bachilo, S. M.; Bondarev, S. L.; Gillbro, T. *J. Photochem. Photobiol., B: Biol.* **1996**, *34*, 39.
(22) Kandori, H.; Sasabe, H. *Chem. Phys. Lett.* **1993**, *216*, 126.
(23) Hamm, P.; Zurek, M.; Röschinger, T.; Patzelt, H.; Oesterhelt D.; Zinth, W. *Chem. Phys. Lett.* **1996**, *263*, 613.
(24) Hamm, P.; Zurek, M.; Röschinger, T.; Patzelt, H.; Oesterhelt, D.; Zinth, W. *Chem. Phys. Lett.* **1996**, *268*, 180.
(25) Froese, R. D. J.; Komaromi, I.; Byun, K. S.; Morokuma, K. *Chem. Phys. Lett.* **1997**, *272*, 335.
(26) Garavelli, M.; Celani, P.; Bernardi, F.; Robb, M. A.; Olivucci, M. *J. Am. Chem. Soc.* **1997**, *119*, 6891.
(27) Becker, R. S.; Hug, G.; Das, P. K.; Schaffer, A. M.; Takemura, T.; Yamamoto, N.; Waddell, W. *J. Am. Chem. Soc.* **1976**, *80*, 2265.
(28) Bondarev, S. L.; Bachilo, S. M. *J. Photochem. Photobiol., A: Chem.* **1991**, *59*, 273.
(29) Becker, R. S.; Freedman, K.; Gausey, G. *J. Am. Chem. Soc.* **1982**, *104*, 5797.
(30) Koyama, Y.; Kubo, K.; Komori, M.; Yasuda, H.; Mukai, Y. *Photochem. Photobiol.* **1991**, *54*, 433.
(31) Mukai, Y.; Imahori, T.; Koyama, Y.*Photochem. Photobiol.* **1992**, *56*, 965.